Topography of lobate scarps on Mercury: New constraints on the planet's contraction

Thomas R. Watters
Center for Earth and Planetary Studies, National Air and Space Museum, Smithsonian Institution, Washington, D.C. 20560
Mark S. Robinson
Department of Geological Sciences, Northwestern University, Evanston, Illinois 60208
Anthony C. Cook
Center for Earth and Planetary Studies, National Air and Space Museum, Smithsonian Institution, Washington, D.C. 20560

ABSTRACT

Lobate scarps are landforms on Mercury that appear to have formed by thrust faulting and are thought to reflect global contraction due to cooling of the planet's interior. Topographic data for 10 mercurian lobate scarps, derived from *Mariner 10* images using photoclinometry and digital stereoanalysis, indicate a range in maximum relief of 0.1 to 1.5 km and a range in horizontal shortening of 0.3 to 3.2 km, assuming fault-plane dips (θ) of 25°. Previous estimates of cumulative compressional strain recorded in the lobate scarps suggest a decrease in Mercury's radius of 1 to 2 km. Our estimate of compressional strain based on these new topographic measurements is ~0.056% (θ = 25°). This suggests that Mercury's radius decreased by <1 km.

INTRODUCTION

Mercurian lobate scarps were first discovered in *Mariner 10* images (Strom et al., 1975). Characterized as features unique in the solar system (Thomas et al., 1988), they are in fact similar in morphology to those found in the highlands of Mars (Watters, 1993; Watters and Robinson, 1996). In plan view, these scarps appear to be one-sided, often lobate, and occur in linear or arcuate segments. They are believed to have formed by thrust faulting on the basis of their morphology and the deformation of crater walls and floors (Strom et al., 1975; Cordell and Strom, 1977; Melosh and McKinnon, 1988; Watters, 1993; Schenk and Melosh, 1994). The compressional stresses that formed the lobate scarps are proposed to have resulted from either global contraction due to secular cooling of the interior, tidal despinning, or a combination of the two (Strom et al., 1975; Cordell and Strom, 1977; Melosh and Dzurisin, 1978; Pechmann and Melosh, 1979; Melosh and McKinnon, 1988). Tidal despinning models, however, predict a system of normal faults at Mercury's poles that has not been observed (see Schubert et al., 1988). The formation of lobate scarps is generally thought to have occurred after the period of heavy bombardment (about 4 Ga), postdating the intercrater plains and the ancient tectonic fabric of the so-called mercurian grid (Strom, 1984; Melosh and McKinnon, 1988).

Moderate-scale mercurian scarps typically have lengths ranging from 20 to 150 km (Strom et al., 1975; Cordell and Strom, 1977; Dzurisin, 1978), and large-scale scarps have lengths >150 km (see Cordell and Strom, 1977, Fig. 3). The largest known lobate scarp on Mercury is Discovery Rupes (Fig. 1; note that only ~45% of Mercury has been imaged). Discovery Rupes is more than 500 km long, and its maximum relief has been estimated to be as low as 1 km and as high as 3 km (Strom et al., 1975; Dzurisin, 1978; Melosh and McKinnon, 1988; Schenk and Melosh, 1994). Although estimates of the dimensions of some of the mercurian lobate scarps are consistent with terrestrial thrust-fault structures (Strom et al., 1975; Cordell and Strom, 1977), the general lack of topographic data for Mercury has made comparisons problematic.

TOPOGRAPHY

Existing topographic data for Mercury have been derived from shadow measurements (Strom et al., 1975; Malin and Dzurisin, 1977; Pike, 1988), photoclinometry (Hapke et al., 1975; Mouginis-Mark and Wilson, 1981; Schenk and Melosh, 1994), point stereoanalysis (Dzurisin, 1978), and Earth-based radar altimetry (Harmon et al., 1986; Harmon and Campbell, 1988). New topographic data for 10 mercurian lobate scarps have been derived from photoclinometry and digital stereoanalysis using updated *Mariner 10* camera orientations (Davies et al., 1996; Robinson et al., 1997) and improved radiometry (Robinson and Lucey, 1997). A digital elevation model of the southern half of Discovery Rupes was generated by digital stereoanalysis (Fig. 2). These data represent the first two-dimensional stereoanalysis of a mercurian lobate scarp.

Digital stereoanalysis involves manually picking a few tie points to act as starting points for the automated stereo matching process, which subsequently finds corresponding points between the images (Day et al., 1992; Thornhill et al., 1993). The image pair coordinates found by the matcher are then fed through a stereo intersection camera model, and the closest point

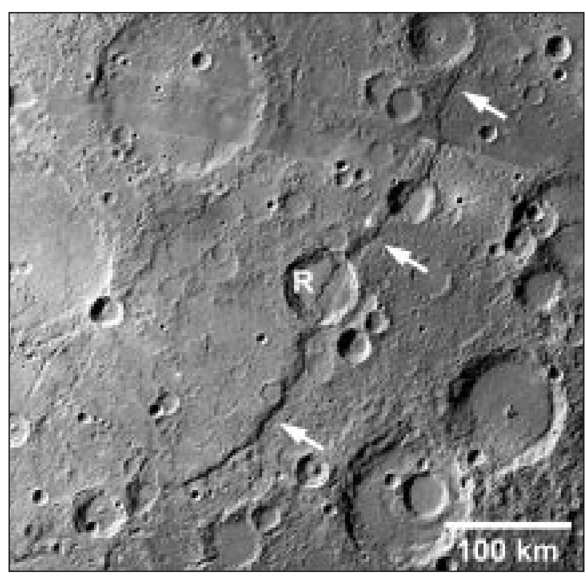

Figure 1. *Mariner 10* mosaic of Discovery Rupes, largest known lobate scarp on Mercury (indicated by arrows). This scarp is ~550 km long and transects 60-km-diameter Rameau crater (R), and smaller 40-km-diameter crater to northeast. Scarp clearly deforms walls and offsets floor materials of two craters.

of intersection specifies the location and elevation of the corresponding ground points. The derived digital elevation model has a grid spacing of 1 km/pixel, and the relative vertical uncertainty of an individual matched point is <500 m. The digital elevation model indicates that Discovery Rupes has a maximum relief of ~1.5 km (Fig. 3). The average relief of the scarp over the general area encompassed by the profiles shown in Figure 3 is 1.3 ± 0.2 km (n = 12). The relief of the southern segment of the scarp is generally <1 km, and the scarp face reaches a maximum slope of ~14°.

Photoclinometry was used to generate topographic profiles across Discovery Rupes and nine other lobate scarps including Santa Maria Rupes (another prominent large-scale scarp; 3.5°N, 19°W). These photoclinometric data provide an independent check of the accuracy of the stereo-derived digital elevation model. Employing the Lommel-Seeliger/Lambert photometric function (McEwen, 1991) that describes the photometric properties of the surface, and two empirically derived parameters, the scattered light value (which corrects for light scattered from surfaces outside a pixel into a given pixel) and the horizontal digital number (the brightness value of a horizontal surface within the image), the slope is recovered and the relative elevation calculated between adjacent pixels (Davis and Soderblom, 1984; Tanaka and Davis, 1988). A comparison of the average maximum relief determined from photoclinometric profiles (n = 10) and profiles extracted from the digital elevation model (n = 5) across the same area of Discovery Rupes indicates that the difference between the two methods is <10% (<100 m). The relief of the other lobate scarps analyzed with photoclinometry ranges from ~0.1 to 0.8 km. An Earth-based radar altimetry profile across Santa Maria Rupes shows that the scarp has a relief of 700 m (vertical uncertainty estimated to be 100 m for a horizontal surface within a resolution cell that is 0.15° longitude by 2.5° latitude or 6 × 100 km; Harmon et al., 1986). Photoclinometric profiles across Santa Maria, in the same location as the radar altimetry, indicate that the relief of the scarp is 712 ± 16 m (the error estimate is based on the variation in elevation for an error in the horizontal digital number of ±2; see Watters and Robinson, 1997).

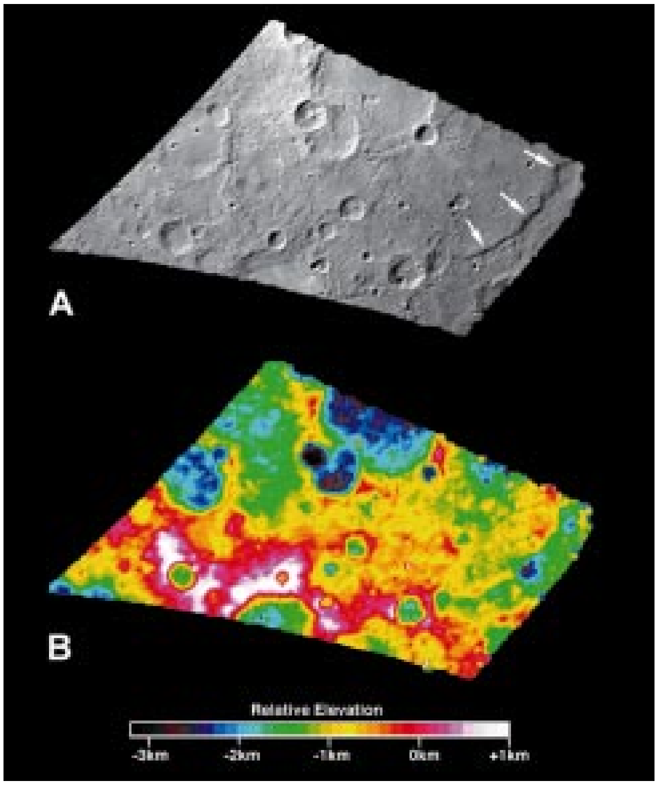

Figure 2. Digital elevation model of southern half of Discovery Rupes. Model was generated using *Mariner 10* stereo pair 27399 and 166613. Area covered by stereo pair is shown in A and the model is shown in B. Shades of blue to black are lows, and shades of red to white are highs. Elevations are relative to 2439.0 km Mercury radius reference sphere. Arrows indicate location of scarp (frame 27399).

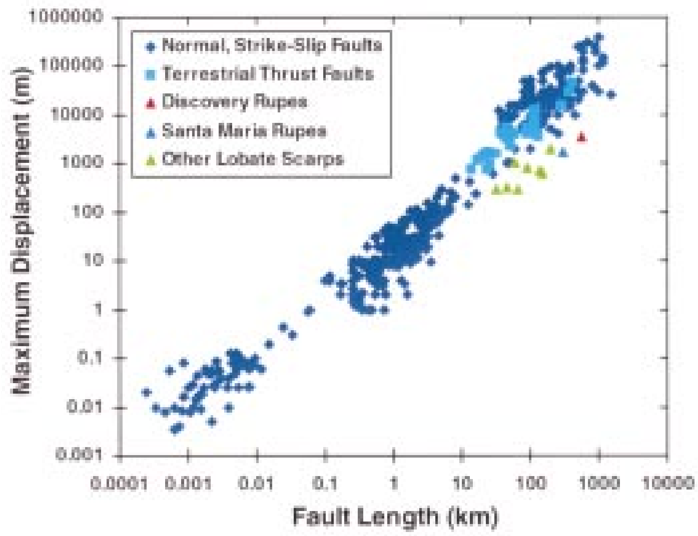

Figure 4. Log-log plot of maximum displacement as function of fault length for terrestrial faults, the faults associated with Discovery Rupes, and nine other lobate scarps on Mercury. Measurements for terrestrial faults are from nine different data sets (including data for 29 thrust faults) (Cowie and Scholz, 1992).

Figure 3. Elevation profiles across Discovery Rupes extracted from digital elevation model (Fig. 2). Lines in A (*Mariner 10* frame 27399) indicate locations of profiles shown in B. Profiles are spaced ~5 km apart. Maximum relief of Discovery Rupes indicated in model is 1532 m (profile A–A′). Elevations are relative to 2439.0 km Mercury radius reference; vertical exaggeration is ~15:1.

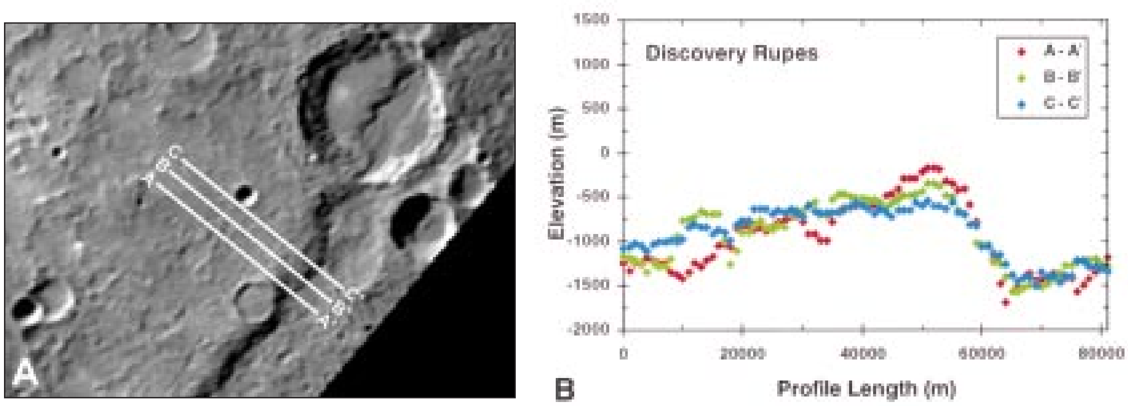

ESTIMATES OF DISPLACEMENT AND HORIZONTAL SHORTENING

The simplest kinematic model for the formation of Discovery Rupes and other mercurian lobate scarps involves deformation associated with a thrust fault that propagates upward and breaks the surface. In this case, the amount of horizontal shortening is estimated assuming that it is a function of the dip of the fault plane and the displacement on the fault. Given the relief of the scarp (h) and the fault-plane dip (θ), the displacement (D) necessary to restore the topography to a planar surface is given by $D = h/\sin\theta$ and the horizontal shortening (S) is given by $S = h/\tan\theta$. The largest uncertainty involved in estimating the displacement and horizontal shortening in this way is the uncertainty in the fault-plane dip.

The optimum angle θ at which faulting will occur is given by $\tan 2\theta = 1/\mu_s$, where μ_s, by analog with ordinary sliding friction, is defined as the coefficient of internal friction (see Jaeger and Cook, 1979). Laboratory data on the maximum shear stress to initiate sliding for a given normal stress for a variety of rock types are best fit by a maximum coefficient of static friction of 0.6 to 0.9 (best fit $\mu_s = 0.85$) (Byerlee, 1978). This suggests that thrust faults will form with dips from about 24° to 30° (~25° for $\mu_s = 0.85$). Field measurements of θ for thrust faults typically range between 20° to 25° (Jaeger and Cook, 1979). However, the Wind River thrust fault in Wyoming has an average θ of 35° that extends to a depth of 36 km with a minimum of 21 km displacement (Brewer et al., 1980) and may have as much as 16 km of throw and 30 km of displacement (M. H. Anders, 1998, personal commun.). Thus it is assumed that thrust faults associated with mercurian lobate scarps will be within a range in θ of 20° to 35°, and the optimum θ is 25°. In the absence of any data to the contrary, it is assumed that fault-plane dips are uniform (i.e., linear, not curved or bent). The Wind River thrust (Brewer et al., 1980) and other thrust faults that cut the Precambrian basement of the Rocky Mountain foreland in Wyoming (Gries, 1983; Stone, 1985) are examples of terrestrial thrust faults that have uniform fault-plane dips that do not significantly steepen or shallow with depth. Some of these thrust faults steepen upward only where they cut Paleozoic sedimentary sequences (Stone, 1985). Using the Wind River thrust fault as an analog with a minimum throw of 12 km (based on 21 km of displacement on the fault), the horizontal shortening estimated using this method is 17 to 33 km for θ in the range of 20° to 35° (~26 km at θ = 25°).

The amount of horizontal shortening across Discovery Rupes based on a maximum relief of 1.5 km and a range in θ of 20° to 35° is 2.1 to 4.1 km (~3.2 km at θ = 25°). The range in horizontal shortening for the other lobate scarps studied is 0.26 to 1.8 km at θ = 25° (n = 9). It is important to note that these estimates assume there has been no significant translation of the fault block over the fault ramp onto the flat. If overthrusting is a significant component of the total horizontal shortening, these estimates are only lower limits. However, there is no significant difference in the diameter of Rameau crater, the larger of two craters cut by Discovery Rupes, regardless of the azimuthal orientation of the measured diameter. These measurements indicate that overthrusting is not a significant component of total horizontal shortening. Of the lobate scarps studied, the only possible exception we have identified is Guido d'Arezzo crater, which is cut by Vostok Rupes (see Dzurisin, 1978).

COMPARISON WITH TERRESTRIAL FAULTS

Field observations of terrestrial faults indicate that a positive correlation exists between the maximum displacement on a fault (D) and the length of the fault trace (L) (Cowie and Scholz, 1992; Gillespie et al., 1992; Dawers et al, 1993; Cartwright et al., 1995). The ratio of displacement to fault length (D/L), defined as γ, ranges between 10^0 and 10^{-3} for terrestrial faults (Cowie and Scholz, 1992). The scatter in the D and L data may reflect the growth of faults by segment linkage where the scaling characteristics change at different stages of fault evolution (Dawers and Anders, 1995; Cartwright et al., 1995; Wojtal, 1996). Cowie and Scholz (1992) suggested that the D-L relationship for continental faults is linear, such that $D = \gamma L$ and γ is determined by rock type and tectonic setting. The value of γ for the mercurian lobate scarps studied (obtained by a linear fit to D-L data, estimates of D being based on θ = 25°) is 6.5×10^{-3}, consistent with the values of γ of terrestrial fault populations (see Cowie and Scholz, 1992). The displacements on the faults associated with lobate scarps are about an order of magnitude lower than those of the terrestrial thrust faults shown in Figure 4. This is likely a reflection of the difference in tectonic setting. Most terrestrial thrust faults are in foreland fold and thrust belts located at convergent plate margins where the structures accumulate large amounts of strain, i.e., the deformation is driven by plate tectonics. By contrast, thrust faulting on Mercury is distributed throughout the crust (Strom et al., 1975; Cordell and Strom, 1977) and is driven by global contraction due to a small change in the radius of the planet.

DISCUSSION

The distributed nature and random orientations of the mercurian thrust faults (Cordell and Strom, 1977) indicate that compressional stresses were global and horizontally isotropic, consistent with compressional stresses resulting from global contraction due to secular cooling. Estimates of the cumulative shortening and the decrease in radius reflected by the lobate scarps are an important constraint on thermal history models for Mercury (Solomon, 1976, 1977; Schubert et al., 1988; Phillips and Solomon, 1997). Thermal history models predict a 2 km decrease in the planet's radius due to secular cooling of the interior (Solomon, 1976, 1977). The first estimate of the decrease in Mercury's radius resulting from global contraction was made by Strom et al. (1975). They determined that the cumulative shortening due to lobate scarp formation resulted in a net decrease in surface area of 6.3×10^4 to 1.3×10^5 km^2, corresponding to a decrease in the radius of Mercury of about 1 to 2 km. The decrease in surface area was estimated by calculating horizontal shortening (S) assuming an average throw of 1 km (based on a range of maximum relief of 0.5 to 3 km) and θ of 45° and 25°, respectively. The resulting S was multiplied by the total length of the scarps (15 150 km) mapped over the area studied (~24% of the surface) to determine the decrease in area, and this decrease was then extrapolated to the entire surface. Adjusting the Strom et al. (1975) estimate using the upper and lower limits for θ applied in this study (35° and 20°), the decrease in surface area becomes 9.09×10^4 to 1.75×10^5 km^2 and the corresponding decrease in radius is about 1.5 to 2.9 km.

We used an alternate method to that employed by Strom et al. (1975) to estimate the decrease in radius. This method involved determining the compressional strain utilizing displacement (D) and length (L) data for the lobate scarps. If the displacement-length scaling relationship of a fault population is known, the strain can be calculated using fault lengths alone (Scholz and Cowie, 1990; Cowie et al., 1993). The strain for large faults ($L \geq$ the maximum depth of faulting) is given by

$$\varepsilon = \frac{\cos(\theta)}{A} \sum_{k=1}^{n} D_k L_k \tag{1}$$

where θ is the fault-plane dip, A is the size of the survey area, n is the total number of faults, and $D = \gamma L$ (Cowie et al., 1993). The lengths of lobate scarps (n = 52) were measured between 70°N and 70°S and 10°W to 90°W, an area covering about 19% of the surface of Mercury. Discovery and Santa Maria Rupes are within the survey area. Over a range in θ of 20° to 35°, the compressional strain is estimated to be between 0.051% and 0.058% (0.056% for θ = 25°). Assuming that the survey area is representative of the entire surface, the corresponding decrease in the radius of the planet is between ~0.62 and ~0.71 km (~0.69 km for θ = 25°). This is below the range estimated by Strom et al. (1975) and predicted by current thermal history models (Solomon, 1976, 1977). Furthermore, the strain is not evenly distributed over the survey area. The compressional strain found in the southern (70°S to 20°S), equatorial (20°S to 20°N), and northern (20°N to 70°N) sections of the survey area is about 0.086%, 0.028%, and 0.058%, respectively (for θ = 25°). Thus the maximum compressional strain is found in the southern section of the survey area where Discovery Rupes is located. Our results suggest that the cumulative compressional strain recorded in the mercurian lobate scarps reflects a decrease in the radius of the planet of <1.0 km, a factor of three less than the upper limit of the previous estimate of the radius decrease. The small amount of post–heavy-bombardment planetary contraction determined in this study (<1.0 km) and the values reported by Strom et al. (1975) (1 to 2 km) are consistent with models that predict Mercury may still have a liquid outer core, as deduced using *Mariner 10* magnetometer results (Schubert et al., 1988; Connerney and Ness, 1988).

ACKNOWLEDGMENTS

We thank Mark H. Anders for his valuable help and insights and Daniel M. Janes for his constructive reviews. We also thank the University College London Laserscan for use of their "Gotcha" stereo-matching software at Deutsches Zentrum für Luft- und Raumfahrt e.V., Berlin. The *Mariner 10* image data was processed using the Integrated Software for Imaging Spectrometers (ISIS), courtesy of U.S. Geological Survey (Flagstaff, Arizona). This research was supported by grants from the National Aeronautics and Space Administration's Planetary Geology and Geophysics Program.

REFERENCES CITED

Brewer, J. A., Smithson, S. B., Oliver, J. E., Kaufman, S., and Brown, L. D., 1980, The Laramide orogeny: Evidence from COCORP deep crustal seismic profiles in the Wind River Mountains, Wyoming: Tectonophysics, v. 62, p. 165–189.

Byerlee, J., 1978, Friction of rocks, *in* Byerlee, J., ed., Rock friction and earthquake prediction: Pure and Applied Geophysics, v. 116, p. 615–626.

Cartwright, J. A., Trudgill, B. D., and Mansfield, C. S., 1995, Fault growth by segment linkage: An explanation for scatter in maximum displacement and trace length data from the Canyonlands grabens of SE Utah: Journal of Structural Geology, v. 17, p. 1319–1326.

Connerney, J. E. P., and Ness, N. F., 1988, Mercury's magnetic field and interior, *in* Vilas, F., Chapman, C. R., and Matthews, M. S., eds., Mercury: Tucson, University of Arizona Press, p. 494–513.

Cordell, B. M., and Strom, R. G., 1977, Global tectonics of Mercury and the Moon: Physics of the Earth and Planetary Interiors, v. 15, p. 146–155.

Cowie, P. A., and Scholz, C. H., 1992, Displacement-length scaling relationship for faults: Data synthesis and discussion: Journal of Structural Geology, v. 14, p. 1149–1156.

Cowie, P. A., Scholz, C. H., Edwards, M., and Malinverno, A., 1993, Fault strain and seismic coupling on mid-ocean ridges: Journal of Geophysical Research, v. 98, p. 17911–17920.

Davies, M. E., Colvin, T. R., Robinson, M. S., and Edwards, K., 1996, Mercury's polar regions: Locations of radar anomalies [ice] [abs.]: American Astronomical Society Bulletin, v. 28, p. 1115.

Davis, P. A., and Soderblom, L. A., 1984, Modeling crater topography from monoscopic Viking orbiter images, 1. Methodology: Journal of Geophysical Research, v. 89, p. 9449–9457.

Dawers, N. H., and Anders, M. H., 1995, Displacement-length scaling and fault linkage: Journal of Structural Geology, v. 17, p. 607–614.

Dawers, N. H., Anders, M. H., and Scholz, C. H., 1993, Growth of normal faults: Displacement-length scaling: Geology, v. 21, p. 1107–1110.

Day, T., Cook, A. C., and Muller, J. P., 1992, Automated digital topographic mapping techniques for Mars: International Archives of Photogrammetry and Remote Sensing, v. 29, p. 801–808.

Dzurisin, D., 1978, The tectonic and volcanic history of Mercury as inferred from studies of scarps, ridges, troughs, and other lineaments: Journal of Geophysical Research, v. 83, p. 4883–4906.

Gillespie, P. A., Walsh, J. J., and Watterson, J., 1992, Limitations of dimension and displacement data from single faults and the consequences for data analysis and interpretation: Journal of Structural Geology, v. 14, p. 1157–1172.

Gries, R., 1983, Oil and gas prospecting beneath Precambrian of foreland thrust plates in Rocky Mountains: American Association of Petroleum Geologists Bulletin, v. 67, p. 1–28.

Hapke, B., Danielson, E., Klaasen, K., and Wilson, L., 1975, Photometric observations of Mercury from *Mariner 10*: Journal of Geophysical Research, v. 80, p. 2431–2443.

Harmon, J. K., and Campbell, D. B., 1988, Radar observations of Mercury, *in* Vilas, F., Chapman, C. R., and Matthews, M. S., eds., Mercury: Tucson, University of Arizona Press, p. 101–117.

Harmon, J. K., Campbell, D. B., Bindschadler, D. L., Head, J. W., and Shapiro, I. I., 1986, Radar altimetry of Mercury: A preliminary analysis: Journal of Geophysical Research, v. 91, p. 385–401.

Jaeger, J. C., and Cook, N. G. W., 1979, Fundamentals of rock mechanics (third edition): London, Chapman and Hall, 593 p.

Malin, M. C., and Dzurisin, D., 1977, Landform degradation on Mercury, the moon, and Mars: Evidence from crater depth/diameter relationships: Journal of Geophysical Research, v. 82, p. 376–388.

McEwen, A. S., 1991, Photometric functions for photoclinometry and other applications: Icarus, v. 92, p. 298–311.

Melosh, H. J., and Dzurisin, D., 1978, Mercurian global tectonics: A consequence of tidal despinning?: Icarus, v. 35, p. 227–236.

Melosh, H. J., and McKinnon, W. B., 1988, The tectonics of Mercury, *in* Vilas, F., Chapman, C. R., and Matthews, M. S., eds., Mercury: Tucson, University of Arizona Press, p. 374–400.

Mouginis-Mark, P. J., and Wilson, L., 1981, MERC: A FORTRAN IV program for the production of topographic data for the planet Mercury: Computers and Geoscience, v. 7, p. 35–45.

Pechmann, J. B., and Melosh, H. J., 1979, Global fracture patterns of a despun planet: Application to Mercury: Icarus, v. 38, p. 243–250.

Phillips, R. J., and Solomon, S. C., 1997, Compressional strain history of Mercury [abs.], *in* Proceedings, Lunar and Planetary Science Conference, 28th: Houston, Lunar and Planetary Institute, p. 1107–1108.

Pike, R. J., 1988, Geomorphology of impact craters on Mercury, *in* Vilas, F., Chapman, C. R., and Matthews, M. S., eds., Mercury: Tucson, University of Arizona Press, p. 165–273.

Robinson, M. S., and Lucey, P. G., 1997, Recalibrated *Mariner 10* color mosaics: Implications for mercurian volcanism: Science, v. 275, p. 197–200.

Robinson, M. S., Davies, M. E., Colvin, T. R., and Edwards, K. E., 1997, A new controlled albedo map of Mercury [abs.], *in* Proceedings, Lunar and Planetary Science Conference, 28th: Houston, Lunar and Planetary Institute, p. 1187–1188.

Schenk, P., and Melosh, H. J., 1994, Lobate thrust scarps and the thickness of Mercury's lithosphere [abs.], *in* Proceedings, Lunar and Planetary Science Conference, 25th: Houston, Lunar and Planetary Institute, p. 1203–1204.

Scholz, C. H., and Cowie, P. A., 1990, Determination of geologic strain from fault slip data: Nature, v. 346, p. 837–839.

Schubert, G., Ross, M. N., Stevenson, D. J., and Spohn, T., 1988, Mercury's thermal history and the generation of its magnetic field, *in* Vilas, F., Chapman, C. R., and Matthews, M. S., eds., Mercury: Tucson, University of Arizona Press, p. 429–460.

Solomon, S. C., 1976, Some aspects of core formation in Mercury: Icarus, v. 28, p. 509–521.

Solomon, S. C., 1977, The relationship between crustal tectonics and internal evolution in the Moon and Mercury: Physics of the Earth and Planetary Interiors, v. 15, p. 135–145.

Stone, D. S., 1985, Geologic interpretation of seismic profiles, Big Horn Basin, Wyoming, Part I: East flank, *in* Gries, R. R., and Dyer, R. C., eds., Seismic exploration of the Rocky Mountain region: Denver, Rocky Mountain Association of Geologists, p. 165–174.

Strom, R. G., 1984, Mercury, *in* Carr, M. H., ed., The geology of the terrestrial planets: NASA Special Paper 469, p. 13–55.

Strom, R. G., Trask, N. J., and Guest, J. E., 1975, Tectonism and volcanism on Mercury: Journal of Geophysical Research, v. 80, p. 2478–2507.

Tanaka, K. L., and Davis, P. A., 1988, Tectonic history of the Syria Planum province of Mars: Journal of Geophysical Research, v. 93, p. 14893–14907.

Thomas, P. G., Masson, P., and Fleitout, L., 1988, Tectonic history of Mercury, *in* Vilas, F., Chapman, C. R., and Matthews, M. S., eds., Mercury: Tucson, University of Arizona Press, p. 401–428.

Thornhill, G. D., Rothery, D. A., Murray, J. B., Cook, A. C., Day, T., Muller, J. P., and Iliffe, J. C., 1993, Topography of Apollinaris Patera and Ma'adim Vallis: Automated extraction of digital elevation models: Journal of Geophysical Research, v. 98, p. 23581–23587.

Watters, T. R., 1993, Compressional tectonism on Mars: Journal of Geophysical Research, v. 98, p. 17049–17060.

Watters, T. R., and Robinson, M. S., 1996, Photoclinometric studies of lobate scarps on Mars [abs.], *in* Proceedings, Lunar and Planetary Science Conference, 27th: Houston, Lunar and Planetary Institute, p. 1391–1392.

Watters, T. R., and Robinson, M. S., 1997, Radar and photoclinometric studies of wrinkle ridges on Mars: Journal of Geophysical Research, v. 102, p. 10889–10903.

Wojtal, S. F., 1996, Changes in fault displacement populations correlated to linkage between faults: Journal of Structural Geology, v. 18, p. 265–279.

Manuscript received April 9, 1998
Revised manuscript received July 17, 1998
Manuscript accepted July 30, 1998